JASA EXPRESS LETTERS ARTICLE asa.scitation.org/journal/jel

Wind- and tidal driven ambient noise in seasonally ice-covered waters north of the Svalbard archipelago

Dag Tollefsen[a] and **Helge Buen**
Norwegian Defence Research Establishment (FFI), Box 115, 3191 Horten, Norway
dag.tollefsen@ffi.no, helge.buen@ffi.no

Abstract: This paper presents analysis of a 1-year (2018–2019) recording of ambient noise (40–2000 Hz) at a seasonally ice-covered location on the continental slope between the Svalbard archipelago and the Nansen Basin, northeast Atlantic Arctic. Time series of ambient noise show highest correlations with ice concentration and wind speed. A log-wind speed regression model is fitted to spectral noise data for three categories of ice concentration. Wind-speed dependence decreases with increasing ice concentration and increases with frequency, except at high ice concentration. Periodicity in noise during the ice-covered season is related to the M2 and M4 tidal current constituents.

[Editor: David R. Barclay] https://doi.org/10.1121/10.0013687

Received: 2 June 2022 **Accepted:** 28 July 2022 **Published Online:** 24 August 2022

1. Introduction

Historic low-frequency acoustic measurements in the Arctic (see overview in Ref. 1) illuminated the specifics of ambient noise (AN) due to ice conditions. Since the historic measurements, the sea ice extent has reduced and comprises younger and thinner ice, which affects noise generating processes.[2] In addition, changes in oceanographic structure, e.g., due to influx of warmer water, can affect AN.[2] Recent studies from ice-covered waters of the Pacific sector of the Arctic Ocean (PAO) (includes the Beaufort Sea, the Chukchi Sea, and the Canada Basin) reveal seasonal variability in AN with local and distant environmental forcing factors.[3–8] Measurements from the Atlantic sector of the Arctic Ocean (AAO) are so far scarce. Early work includes a few seasonal data sets;[9–11] recent work includes data from a drifting buoy,[12] and short- and long-term observations in the Fram Strait.[13,14] One may presume that noise-generating processes are similar across the Arctic; however, AN and its relation to forcing factors may differ due to ice extent and ice composition. Also, AN in the PAO is now affected by seasonal inflow of warm Pacific water creating a subsurface sound speed duct that can provide for low-loss long-range propagation and increased influence of distant generated noise.[5–7] In the AAO, increase in the distribution of warm Atlantic water[15] can potentially affect AN in a similar manner, although such effects have yet to be observed.

This paper focuses on two aspects of AN in the presence of ice cover: (1) wind-speed dependence, and (2) periodicity in noise. Regression equations that relate AN to wind speed have been established from open-water data,[16,17] while for ice-covered waters,[3–7] this has to date been less explored. We fit a log-wind speed regression model to spectral noise data for different categories of ice concentration. Periodicity has been observed in historic data and related to factors including sea ice motion[9] and atmospheric forcing;[18] recent shallow-water measurements from the PAO find strong relation to tidal forcing.[4,8] We observe noise periodicity that aligns with tidal current constituents in the AAO.

2. Data and processing

2.1 Experiment area

The acoustic data were collected with a hydrophone at 1155 m depth, located at 1365 m water depth at nominal position 81° 30′ N 26° E, approximately 60 nmi north of the Svalbard archipelago. The site, Fig. 1(a), is on a slope between the continental shelf north of Svalbard (depths 50–200 m) and the deep Nansen Basin (depths to 4000 m) of the northeast Atlantic sector of the Arctic Ocean. A seasonal cover of predominantly first-year ice characterizes ice conditions in the area (Renner *et al.*[19] measured sea ice thickness in the area and found a heavy-tailed distribution over 0–4 m with a mode at 1.2 m). Oceanographic conditions are dominated by the Svalbard Branch of the Western Spitsbergen Current, carrying warm Atlantic water eastward along the shelf, partially mixing in with cold polar water from the north.[20]

Observations of marine mammals north of Svalbard include bowhead whale, ringed seal, bearded seal, and walrus.[21] Seasonal presence of larger cetaceans include fin and blue whale,[22] while signatures due to sperm and bowhead

[a]Author to whom correspondence should be addressed.

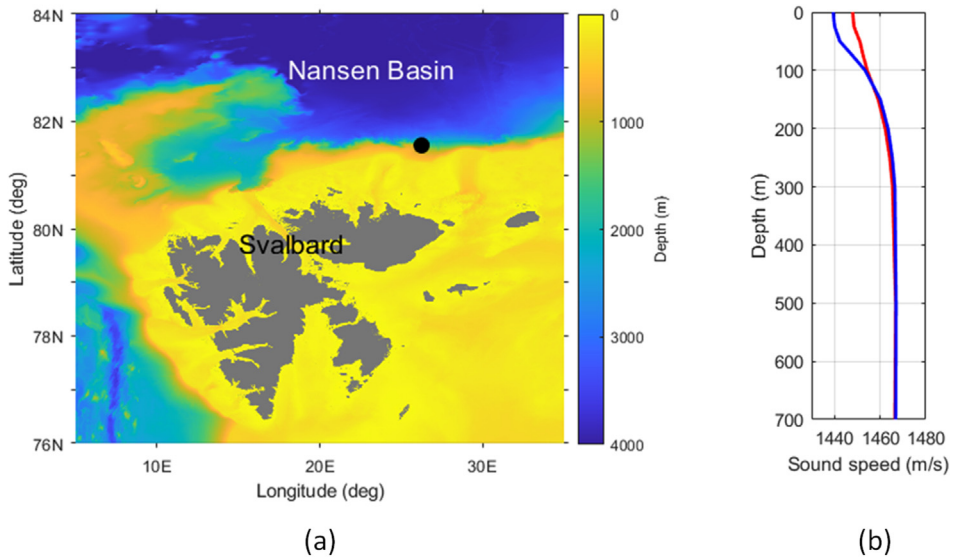

Fig. 1. (a) Area and site of experiment (black dot). Color code is water depth in m. (b) Average model sound speed versus depth for ice-free (red) and ice-covered (blue) seasons.

whale have been observed in the adjacent Fram Strait.[13,14] Shipping activity due to fishing and tourism is sporadic in periods of ice-free waters.[23]

2.2 Environmental model data

Environmental model data were accessed from The Norwegian Meteorological Institute (met.no).[24] This included the regional ocean modeling system (ROMS) Barents-2.5 km coupled ocean–sea ice model (grid size 2.5 km) for daily mean ocean current, temperature and salinity versus depth, and daily mean sea ice concentration, the regional wave model (WAM) Nordic Seas (4 km) for hourly wind speed and ocean wave data, and the AROME Arctic (2.5 km) weather model (3 h resolution) for air pressure and temperature.

Figure 1(b) shows averaged ocean sound speed profiles for two seasons (average over daily mean ROMS model profiles at the closest grid point). During the ice-covered season (March to September), cold polar water (−1.45 °C to −1.78 °C) forms an upper layer approximately 100 m thick. This layer vanishes during the ice-free season when warm Atlantic water (+0.2 °C to +1 °C) dominates. The upper layer reduces potential influence of distant surface-generated noise in the ice-covered season due to increased under-ice propagation loss.

2.3 Acoustic data and processing

The acoustic data were collected with an M36-V30-100 hydrophone (GeoSpectrum Inc., Canada) attached to an AMAR-G4-UD recording instrument (Jasco Applied Sciences, Canada). The hydrophone sensitivity was −164.7 dB re 1 V/μPa (factory calibrated prior to instrument delivery) with a high-pass filter at 20 Hz before 24 bit digitization. The hydrophone self-noise is 46 dB re μPa at 100 Hz and 36 dB re μPa at 1 kHz. The AMAR instrument was fitted in-line to a lightweight rig, bottom moored at 1365 m water depth. The instrument recorded at 33% duty cycle: 16 kHz sampling for 20 min. each 2 of 3 h, and 64 kHz for 20 min. each third hour, from October 21, 2018 to October 25, 2019.

Tidal-induced flow noise (FN) due to pressure and velocity fluctuations around the surface of a hydrophone has been reported in high-flow (∼3 m/s) coastal and shallow-water tidal channels.[25] FN was predicted using the mean-flow model of Bassett *et al.*:[25] for a current speed of 0.3 m/s (ROMS yearly maximum), FN is above the hydrophone self-noise up to ∼40 Hz. Though mitigated by a custom flow shield, data below 40 Hz were excluded from further analysis.

For noise power spectral density (PSD) estimation, we used the Welch method with 1 min averages over 1 s fast Fourier transform (FFT) samples (Hamming windowed with 50% overlap). This resulted in 480 noise spectra per day, of 1 min duration. Resulting PSD noise levels are in units of dB re 1 μPa^2/Hz. To also estimate a persistent background noise level,[16] data were processed by a procedure adopted from Kinda *et al.*[4] and Bonnel *et al.*[6] We then used short-term FFTs (a sliding time window of length 64 ms and 50% overlap; 15 Hz–wide frequency bins) over the first 7 min of data from each hour. The resulting ambient noise levels (ANL) in dB re 1 μPa^2/Hz were estimated from the lowest 15th percentile in each frequency bin.

3. Results

3.1 Long-term spectrogram and ice conditions

Figure 2(a) shows daily ice concentration (IC) at the sensor location (in %) and range to the ice edge (in km, defined by 15% IC). Data are in the following grouped by IC into three categories: *relatively open water* (IC < 15%), *nearly full ice cover* (IC > 85%), and *intermediate ice conditions* (IC 15%–85%). There are *relatively open-water* conditions through mid-November, in mid-December, and again for a short period in February. There is *nearly full ice cover* from mid-March through July. The number of days within each category is 69, 147, and 153, respectively.

Figure 2(b) presents the long-term spectrogram of ANL (40 Hz to 2 kHz). Overall, the spectrogram displays known seasonality observed from ice-covered waters elsewhere: high ANL during periods of open water and partial ice cover, and lower ANL (by 15–20 dB) in periods of ice cover. Note several intermittent shorter-term periods (duration 1–3 days; e.g., in mid-January and early February) of elevated ANL (by 6–12 dB) that coincide with proximity to the ice edge.

3.2 Correlations with environmental factors

Correlation analysis was applied to time series of noise (hourly median noise PSD, power-sum over the 0.1–1 kHz band) and environmental factors (data taken from met.no models at the nearest grid geographical position, up-sampled to 1 h resolution where available at lower resolution). For the 369 day–long data set, the highest correlations were with wind speed (Pearson's correlation coefficient $r = 0.65$) and IC ($r = -0.51$), followed by ocean surface current ($r = 0.32$) and air pressure ($r = -0.24$) (all p-values $p < 0.001$). Alternative parameterizations for ice conditions, including IC within a 100 km radius, and range to the ice edge, as well as time lags (up to ±2 days) between noise and environmental factors were applied but did not significantly alter the correlation values over those reported here.

3.3 Wind-speed dependence

In ice-covered waters, ice tends to reduce noise due to surface agitation while additional noise can be generated by colliding and contacting ice floes.[16] Correlation between wind speed (WS) and low-frequency AN has been observed and quantified in recent data from seasonally ice-covered waters of the PAO,[3,6,7] but there is no well-established noise/wind speed model as for open water.

We adopt a model based on the composite wind-related surface noise model proposed by Ainslie:[26]

$$NL = O(f) + 20n(f)\log_{10} v - 10\log_{10}\left[1.5 + \left(\frac{f}{1000}\right)^{1.59}\right], \quad (1)$$

with the noise level (NL) at frequency f (in dB re μPa^2/Hz), $O(f)$ an offset parameter, and $n(f)$ the slope of the log-dependence on wind speed v (in m/s, at 10 m height). (A temperature-dependent term and additional depth-dependent correction terms in the Hildebrand open-water model[17] were evaluated to <1 dB and were hence omitted.)

Figures 3(a) and (b) present noise level (hourly median spectral PSD) versus WS at 250 Hz and 1 kHz, for the three classes of IC. Wind speed is here the hourly values taken from the WAM mode. (Data at $v < 2$ m/s were plotted but were not used in the regression.) Table 1 lists the coefficients of the regression equation, Eq. (1), and the correlation

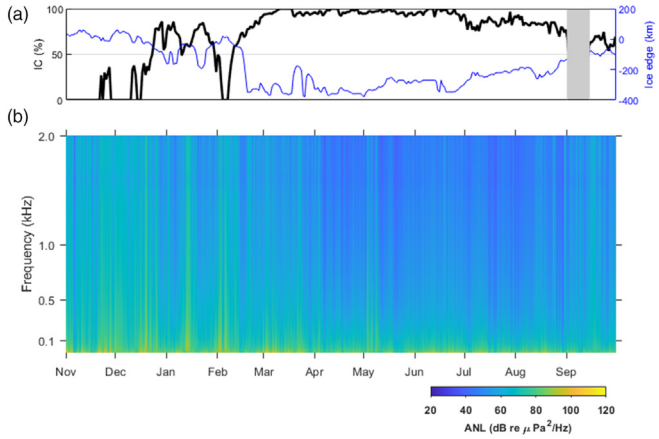

Fig. 2. (a) Ice concentration (IC, in %) and range to ice edge (km, negative for IC > 15%), (b) long-term spectrogram of ANL (November 2018 to October 2019).

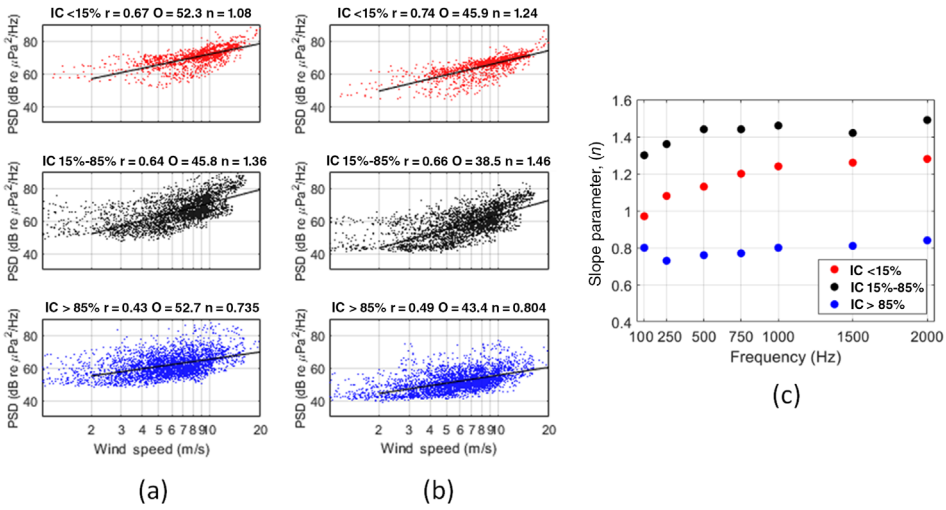

Fig. 3. Noise PSD (dB re μPa^2/Hz) versus WS (m/s) for three categories of IC at (a) 250 Hz, and (b) 1 kHz. Color code is IC <15% (red), IC 15–85% (black), and IC >85% (blue). Solid line is regression model [Eq. (1)] fit to data for WS 2–20 m/s. Correlation coefficient (r) and model coefficients (O and n) indicated above each panel. (c) Regression model slope (n) versus frequency, for three categories of IC.

coefficients ($p < 0.001$). For comparison, coefficients for the Ainslie open-water model and a regression model fit at 250 Hz for two classes of IC from Ref. 3 are included in the table.

For *relatively open water* (IC < 15%), which includes days of fully open-water conditions, model correlation is high (0.67 and 0.74, respectively, at 250 Hz and 1 kHz). Both the 250 Hz and 1 kHz model coefficients are close to the Ainslie model. The slope coefficient is, however, twice that found in Ref. 3; possibly due to differences in proportions of open-water data between the data sets. For *nearly full ice cover* (IC > 85%), the correlation is low (0.43 and 0.49, respectively). The offset parameter is comparable to that found for low IC; however, the slope parameter is reduced by approximately *one-third* (at 250 Hz from 1.08–0.74, at 1 kHz from 1.24–0.80). This indicates significantly less WS dependence with ice cover, in agreement with previous observations. For *intermediate* conditions (IC 15%−85%), the correlation is overall high (∼0.65), with lower offset parameters but higher slope parameters than for low IC. This category comprises a larger variety of ice conditions.

Figure 3(c) presents the slope parameter obtained by fitting Eq. (1) to data at frequencies of 100, 250, 500, 1000, and 2000 Hz. Consistent with observations from open-water data,[17] the slope parameter increases with frequency, at least for the two lowest categories of IC. However, for *nearly full ice cover*, the model slope is near constant with frequency.

3.4 Tidal forcing

Periodicity in NL with tidal constituents was observed by Kinda *et al.*,[4] who found elevated NL (at 10–500 Hz) with periodicity concurrent with tidal components M2 (0.26 days) and M4 (0.52 days). More recently, Cook *et al.*[8] found periodicity in NL at 63 Hz and 1.5 kHz coinciding with the M2 and several other tidal components.[8] Both these data sets were from shallow-water sites in the PAO.

Table 1. IC, frequency, regression model [Eq. (1)], and correlation coefficient for model fit to noise PSD data at 250 Hz and 1 kHz.

IC (%)	Frequency (Hz)	$O(f)$	$n(f)$	r
Open water (Ref. 26)	250	44.3	1.12	
	1000	42.2	1.12	
<15	250	52.3	1.08	0.67
15–85	250	45.8	1.36	0.64
>85	250	52.7	0.74	0.43
<15	1000	45.9	1.24	0.74
15–85	1000	38.5	1.46	0.66
>85	1000	43.4	0.80	0.49
Roth (Ref. 3)				
<25	250	58.4	0.49	0.62
>75	250	52.4	0.25	0.28

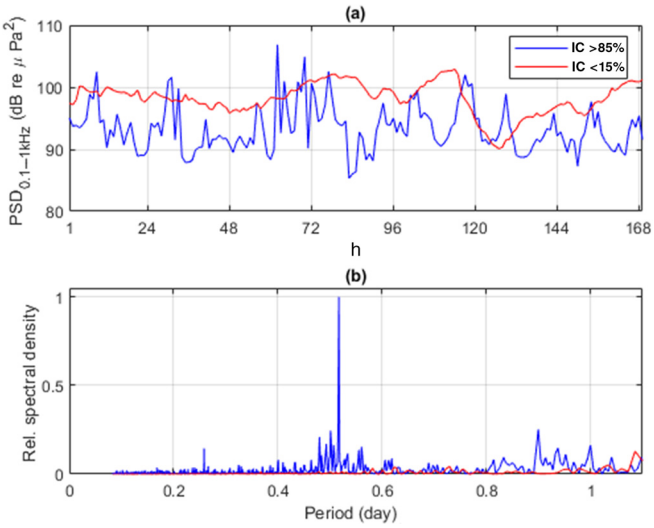

Fig. 4. (a) 7 day time series of noise PSD (0.1–1 kHz) during IC < 15% (red) and IC > 85% conditions (blue). (b) Spectra of noise time series during a 2 month period of IC < 15% (red) and a 5 month period of IC > 85% (blue).

Figure 4(a) shows hourly noise PSD (0.1–1 kHz) for two 1 week periods, starting November 10 (IC < 15%), and March 5 (IC < 15%), respectively. The 24 h variation in noise levels is up to 15 dB during both periods. Figure 4(b) shows the power spectra of hourly PSD time series during periods of low IC (2 month period starting November 1) and high IC (5 month period starting March 1). The highest spectral peak at 0.5172 days (12.41 h) coincides with the M2 *principal lunar semidiurnal* tidal component. Less prominent secondary peaks can be observed at 0.2586 days (6.21 h) which coincides with M4 *shallow-water overtide of M2*, and at 0.5015 days (12.03 h), which coincides with the S2 *principal solar semidiurnal* component. Peaks are observed *only* in the ice-covered period. Regional differences in tidal influence on noise can be expected. An Arctic tidal current atlas[27] identifies M2 and S2 as two dominant components at a nearby site on the continental slope in the AAO; in the PAO, the M2 and K1 components are strongest. This may in part explain differences in observed tidal periods between data sets. Semi-diurnal periodicity can secondarily be induced by wind-driven currents; however, this effect is less prevalent with depth and reduces with increasing ice cover.[27]

4. Summary

This paper examined ambient noise data collected under seasonal ice cover on the continental slope north of the Svalbard archipelago in the Northeast Atlantic sector of the Arctic, an area so far less surveyed for present-day noise conditions. The 1-year spectrogram of ANL showed a typical seasonality with ice conditions: high ANL during periods of open water and lower ANL by 15–20 dB in periods of ice cover.

A log-wind speed model yielded good correlation with noise spectral data for high ice concentration (IC > 85%). The model slope significantly reduced (halved) from low (IC < 15%) to high ice concentration, consistent with a dampening effect of the ice cover on surface-generated sound. The model slope was highest for intermediate conditions (IC 15%−85%), possibly indicating a stronger forcing effect of wind due to moving and/or colliding ice floes. During low IC, the model slope increased with frequency (0.1–2 kHz), consistent with the open-water model. For high IC, model slope was near constant with frequency. Finally, periodicities in noise levels that aligned with M2, S2, and M4 tidal constituents were observed during the period of high IC, comparable to recent observations from the PAO.[8]

Acknowledgments

The authors would like to thank the crews of the R/V H U SVERDRUP II and the RNCGV SVALBARD for assistance in rig deployment and recovery.

References and links

[1]E. D. Cook, D. R. Barclay, and C. G. Richards, "Ambient noise in the Canadian arctic," in *Governance of Arctic Shipping*, edited by A. Chircop, F. Goerlandt, C. Aporta, and R. Pelot (Springer Polar Sciences, Cham, 2017), pp. 105–133.
[2]P. F. Worcester, M. A. Dzieciuch, and H. Sagen, "Ocean acoustics in the rapidly changing Arctic," Acoust. Today **16**, 55–64 (2020).
[3]E. Roth, J. A. Hildebrand, and S. M. Wiggins, "Underwater ambient noise on the Chukchi Sea continental slope from 2006–2009," J. Acoust. Soc. Am. **131**, 104–110 (2012).
[4]G. B. Kinda, Y. Simard, C. Gervaise, J. I. Mars, and L. Fortier, "Under-ice ambient noise in Eastern Beaufort Sea, Canadian Arctic, and its relation to environmental forcing," J. Acoust. Soc. Am. **134**, 77–87 (2013).

[5]R. Chen and H. Schmidt, "Temporal and spatial characteristics of the Beaufort Sea ambient noise environment," J. Acoust. Soc. Am. **148**, 3928–3941 (2020).
[6]J. Bonnel, G. B. Kinda, and D. P. Zitterbart, "Low-frequency ocean ambient noise on the Chukchi Shelf in the changing Arctic," J. Acoust. Soc. Am. **149**, 4061–4072 (2021).
[7]M. Ballard and J. Sagers, "Clustering analysis of a yearlong record of ambient sound on the Chukchi Shelf in the 40 Hz to 4 kHz frequency range," J. Acoust. Soc. Am. **150**, 1597–1608 (2021).
[8]E. D. Cook, D. R. Barclay, and C. G. Richards, "Real-time acoustic observations in the Canadian Arctic Archipelago," J. Acoust. Soc. Am. **151**, 1607–1614 (2022).
[9]R. S. Pritchard, "Sea ice noise-generating processes," J. Acoust. Soc. Am. **88**, 2830–2842 (1990).
[10]N. C. Makris and I. Dyer, "Environmental correlates of Artic ice-edge noise," J. Acoust. Soc. Am. **90**, 3288−3298 (1991).
[11]R. H. Bourke and A. R. Parsons, "Ambient noise characteristics of the northwestern Barents Sea," J. Acoust. Soc. Am. **94**, 2799–2808 (1993).
[12]E. Ozanich, P. Gerstoft, P. F. Worcester, M. A. Dzieciuch, and A. Thode, "Eastern Arctic ambient noise on a drifting vertical array," J. Acoust. Soc. Am. **142**, 1997–2006 (2017).
[13]F. Geyer, H. Sagen, G. Hope, M. Babiker, and P. F. Worcester, "Identification and quantification of soundscape components in the marginal ice zone," J. Acoust. Soc. Am. **139**, 1873–1885 (2016).
[14]H. Ahonen, K. M. Stafford, L. de Steur, C. Lydersen, Ø. Wiig, and K. M. Kovacs, "The underwater soundscape in western Fram Strait: Breeding ground of Spitsbergen's endangered bowhead whales," Mar. Poll. Bull. **123**, 97–112 (2017).
[15]I. V. Polyakov, A. V. Pnyushkov, M. B. Alkire, I. M. Ashik, T. M. Baumann, E. C. Carmackilona Goszczko, J.Guthrie, V. V. Ivanov, T. Kanzow, R. Krishfield, R. Kwok, A. Sundfjord, J. Morison, R.Rember, and A. Yulin, "Greater role for Atlantic inflows on sea-ice loss in the Eurasian Basin of the Arctic Ocean," Science **356**, 285–291 (2017).
[16]W. M. Carey and R. B. Evans, *Ocean Ambient Noise* (Springer, New York, 2011).
[17]J. A. Hildebrand, K. E. Frasier, S. Baumann-Pickering, and S. M. Wiggins, "An empirical model for wind-generated ocean noise," J. Acoust. Soc. Am. **149**, 4516–4533 (2021).
[18]J. K. Lewis and W. W. Denner, "Arctic ambient noise in the Beaufort Sea: Seasonal relationships to sea ice kinematics," J. Acoust. Soc. Am. **83**, 549–565 (1988).
[19]A. H. H. Renner, S. Hendricks, S. Gerland, J. Beckers, C. Haas, and T. Krumpen, "Large-scale ice thickness distribution of first-year sea ice in spring and summer north of Svalbard," Ann. Glaciol. **54**, 13–18 (2013).
[20]M. D. Pérez-Hernández, R. S. Pickart, V. Pavlov, K. Våge, R. Ingvaldsen, A. Sundfjord, A. H. H. Renner, D. J. Torres, and S. Y. Erofeeva, "The Atlantic Water boundary current north of Svalbard in late summer," J. Geophys. Res. Oceans **122**, 2269–2290, https://doi.org/10.1002/2016JC012486 (2017).
[21]C. D. Hamilton *et al.*, "Marine mammal hotspots across the circumpolar Arctic," Divers. Distrib. **00**, 1–25 (2022).
[22]H. Ahonen, K. M. Stafford, C. Lydersen, C. L. Berchok, S. E. Moore, and K. M. Kovacs, "Interannual variability in acoustic detection of blue and fin whale calls in the Northeast Atlantic High Arctic between 2008 and 2018," Endanger. Species Res. **45**, 209–224 (2021).
[23]A. N. Stocker, A. H. H. Renner, and M. Knol-Kauffman, "Sea ice variability and maritime activity around Svalbard in the period 2012–2019," Nat. Sci. Rep. **10**, 17043 (2020).
[24]Information on environmental model data from The Norwegian Meteorological Institute available at https://www.met.no/en (Last viewed May 31, 2022).
[25]C. Bassett, J. Thomson, P. H. Dahl, and B. Polagye, "Flow-noise and turbulence in two tidal channels," J. Acoust. Soc. Am. **135**, 1764–1774 (2014).
[26]M. A. Ainslie, *Principles of Sonar Performance Modeling* (Springer, Berlin, 2010), p. 426, Eq. (8.206).
[27]T. M. Baumann, I. V. Polyakov, L. Padman, S. Danielson, I. Fer, M. Janout, W. Williams, and A. N. Pnyushkov, "Arctic tidal current atlas," Sci. Data **7**, 275 (2020).